2

Characterization Techniques for Nanoparticles

Dilawar Hassan[1] , Ahmed El-mallul[2,3]

[1]Tecnologico de Monterrey, School of Engineering and Sciences, Atizapan de Zaragoza, Estado de Mexico 52926, Mexico
[2]University of Radom. Radom -Poland
[3]Al Zentan University. Al Zentan -Libya

Outline

Introduction

Nanomaterials have long been researched for their biomedical potential and various articles have been published in past 2 decades [1]. For to use the nanoparticles to study their biomedical properties or to evaluate their pharmacognostic potential, nanoparticles have to be in specific size range and should possess specific morphological and physiochemical orientation [2-4]. To evaluate these properties various instruments have been developed over the time, that can help scientists and researchers to evaluate the crystalline nature, size range, topographic and tomographic, optical, magnetic and biomedical characteristics of the synthesized nanoparticles. **Table 2.1** shows the list of various properties of nanoparticles with the name of characterization instrument that may be used for that property evaluation.

TABLE 2.1
Instruments used for studying various properties of nanoparticles and biological imaging (i.e., tumor, nanoparticles in an animal model, cell cultures), ideas taken from [5].

Property	**Characterization Instrument**
Shape / Size (Morphology)	Scanning / Transmission Electron Microscopy
	Dynamic Light Scattering
	Confocal LASER Microscopy
	Atomic Force Microscopy
Chemical Composition	Fourier Transform Infrared Spectroscopy
	Electron Dispersive X-ray Spectroscopy
Surface / Crystallinity	Bruauer-Emmett-Teller
	X-ray Diffraction
Optical	RAMAN Spectroscopy
	UV Visible Spectrophotometry
	Surface Plasmon Resonance
Biological	Magnetic Resonance Imaging
	Ultrasound Imaging

To evaluate a nanoparticle's biomedical properties, a nanoparticle must be properly characterized, yet characterizing using all the techniques is a tough task. Since over time, nanoparticles may develop various changes, due to magnetic and other interactions.
Herein, we will, briefly, look into the working principle of various instruments used for characterizing a nanoparticle.

UV Visible Spectrophotometry (UV-Vis)

UV visible Spectrophotometry spectroscopy is a type of absorption spectroscopy, where molecules absorb light in the UV and visible region (190–800 nm). UV spectroscopy covers electromagnetic

radiation between 190 and 800 nm, divided into the UV (190–400 nm) and visible (400–800 nm) regions [6]. **Figure 2.1** shows the schematics of UV-Visible spectrophotometry.

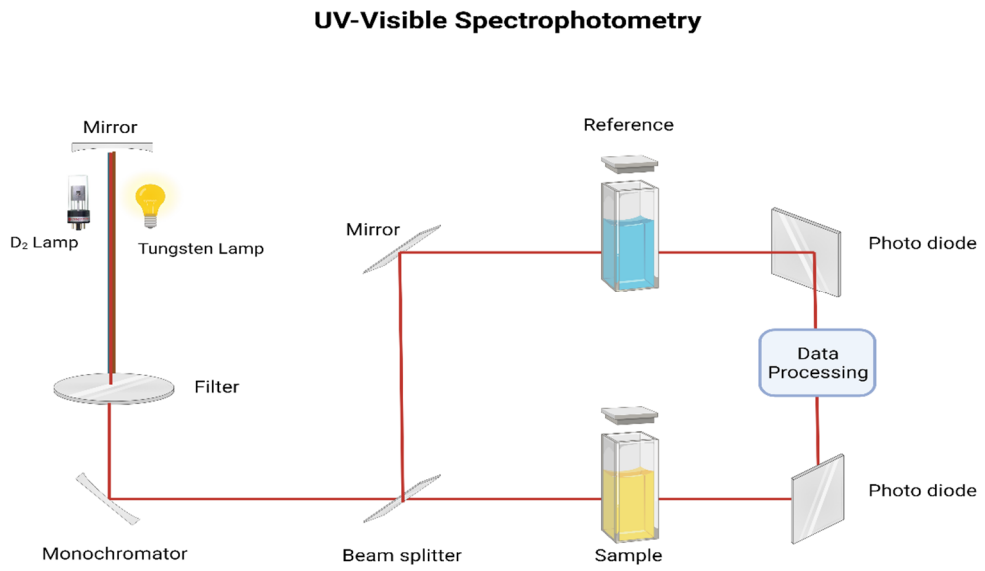

FIGURE 2.1
Schematic of UV-Visible Spectrophotometry working principle.

As the absorption of UV or visible radiation induces transitions between electronic energy levels, it is also known as electronic spectroscopy [7]. Depending on the excitation of electrons, from the ground state to the excited state, once they absorb the light wave. The value of energy absorbed directly corresponds to the change of energy between ground and excited states [8]. Mathematically represented as:

$\Delta E = h\nu$

Typically, the preferred transition is from the highest occupied molecular orbital to the lowest unoccupied molecular orbital. This electron transfer can occur in transition metal ions (d-d transitions and ligand-to-metal or metal-to-ligand charge transfer transitions) and inorganic and organic molecules (mainly $\pi \rightarrow \pi^*$ and $n \rightarrow \pi^*$ transitions) [6]. The Beers-Lambert law governs UV spectroscopy, stating that The Beer-Lambert law, also known as Beer's law, expresses the linear relationship between the concentration of a solute in a solution, the path length of the sample through which light passes, and the absorbance of the light by the solute. Mathematically, it can be represented as:

$A = \varepsilon \cdot c \cdot l$

Where:

- A is the absorbance of the solution,

- ε is the molar absorptivity (also known as molar extinction coefficient or molar absorption coefficient) of the solute,
- c is the concentration of the solute,
- l is the path length of the sample.

This relationship holds true under certain conditions, such as the solute following the Beer-Lambert law and the absence of significant scattering or re-emission of light within the sample. The law is widely used in UV-visible spectrophotometry and other absorption techniques for quantitative analysis of the concentration of absorbing species in a sample. This equation quantifies the relationship between absorbance, concentration, and path length in UV spectroscopy.

Applications

UV-visible spectroscopy finds routine applications in analytical chemistry, serving for the quantitative determination of various analytes. Common applications include:

- Quantitative Determination: Used for quantifying analytes such as transition metal ions, highly conjugated organic compounds, and biological macromolecules.
- Nanoparticle Size and Concentration: Applied to determine the size and concentration of nanoparticles (NPs).
- Evaluation of Nanoparticle Aggregation: Employed to assess the extent of aggregation of nanoparticles.

Monitoring Stability of NP Solutions: UV-visible spectroscopy serves as a simple and reliable method for monitoring the stability of nanoparticle solutions. Changes in the extinction peak intensity or the emergence of secondary peaks at longer wavelengths indicate variations in stability. As nanoparticles destabilize, the original extinction peak may decrease due to the depletion of stable nanoparticles, and additional features like peak broadening or secondary peaks may arise, signalling the formation of aggregates.

Fourier Transform Infrared Spectroscopy (FTIR)

The interaction of IR (infrared) electromagnetic radiation with molecules distinguishes itself from UV-vis (ultraviolet-visible) and X-rays, as it does not excite electrons to higher energy states [9]. Instead, IR radiation amplifies molecular and rotational vibrations without involving electronic transitions [10]. In the far IR region (lower energy toward 400,000 nm), changes induced by rotational vibrations are quantified, while the near IR region (toward 700 nm) includes both vibrational-rotational vibrations [11]. In IR spectroscopy, the absorption frequency varies with vibrational modes, and the intensity depends on the efficiency of molecules in absorbing energy, contingent upon the change in the dipole moment [12]. **Figure 2.2** shows the schematics of operating system of FTIR.

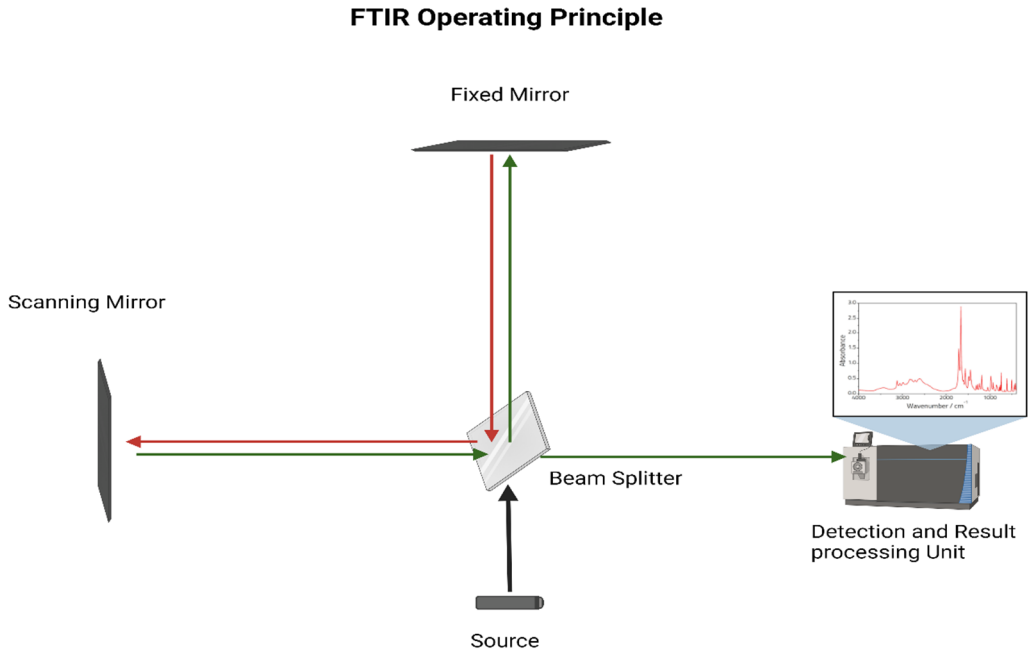

FIGURE 2.2
Operating system of FTIR.

Symmetrical molecules like diatomic gases (e.g., N2, H2, O2) lack a dipole moment, resulting in the absence of a characteristic IR spectrum fingerprint [13]. Two primary vibrational modes are stretching and bending. Stretching vibrations involve an atom's movement within the bond axis without altering the bond angle [14]. In symmetrical stretching, atoms move uniformly away from or toward the central atom, whereas in asymmetrical stretching, one atom approaches the central atom while the other moves away [15]. Bending vibrations, conversely, involve movement related to atoms bonded to a central atom, leading to a change in bond axis and angle [16]. Various bending vibrations, including rocking and scissoring vibrations within the molecular plane, and wagging and twisting vibrations moving out of the plane, contribute to the overall spectrum.

The stretching vibrational frequency adheres to Hook's law, describing the potential on an ideal spring [11]. According to Hook's law, the vibrational frequency of a bond is directly proportional to the bond strength and inversely proportional to the mass. Significantly, the stretching vibration of a triple bond exhibits a higher frequency than double or single bonds, and the vibrational frequency is inversely proportional to the mass of the atoms [10].

Table 2.2 shows the information about the peak values that we can get after analysing a sample through FTIR and how can we interpret the results using those values.

TABLE 2.2
Absorption band /Peak values obtained from FTIR spectrum and the interpretation of those values.

Absorption Band / Peak (cm^{-1})	**Functional Group**
3350-3200	O – H Stretching (Alcohol)
3700-3100	O – H Stretching (Water)
3000-2500	O – H Stretching (Carboxylic Acid)
2950-2850	C – H Stech (Alkyl)
3100-3010	C – H Stech (Alkenyl)
3300	C – H Stech (Alkynyl)
3030	C – H Stech (Aromatic)
3500-3350	N – H Strech
1680-1620	C = C Strech (Alkenyl)
2260-2100	C ≡ C Strech (Alkynyl)
1700-1500	C = C bending (Aromatic)
860-680	C – H Bending (Aromatic)
2260-2220	C ≡ N Strech (Nitrile)
1740-1715	C = O (Aldehyde)
1600	NO_x Strech
1250-1050	C – O – C Strech

XRD

The pivotal discovery of X-rays by Wilhelm Conrad Roentgen in 1895 marked a transformative moment in the scientific landscape, setting the stage for significant advancements in various disciplines [17]. Roentgen's groundbreaking work not only opened the door to new medical applications but also laid the groundwork for technological innovations. A key development stemming from this discovery was the research on X-ray diffraction (XRD) initiated by Laue, Friedrich, and Knipping in 1912, presenting fresh avenues for exploring crystalline materials [18].
In the subsequent years, X-ray methods have undergone substantial evolution, emerging as powerful tools in the realms of materials science and engineering. These methods, rooted in X-rays, can be broadly classified into three main categories:

X-ray Fluorescence Spectroscopy (XRF) [19]:

- Widely employed for both qualitative and quantitative chemical analysis.

- Particularly prevalent in the context of electron microscopes.

X-ray Radiography and Computer Tomography [20]:

- X-ray radiography involves imaging based on the intensity passing through an object, providing insights into its internal structure.
- X-ray computer tomography represents a significant advancement, enabling detailed three-dimensional imaging.

X-ray Diffraction (XRD) Methods [21]:

- Leverage the unique ability of crystals to diffract X-rays, facilitating a precise examination of crystalline phase structures.
- Recorded diffraction patterns encompass contributions from various micro- and macrostructural features of a sample.
- Key investigation parameters include peak position, lattice parameters, space group, chemical composition, macro-stresses, and qualitative phase analysis.
- Peak intensity yields information about crystal structure, including atomic positions, temperature factor, or occupancy, as well as texture and quantitative phase analyses.
- Peak shape provides insights into sample broadening contributions, such as micro-strains and crystallite size [21].

In the domain of materials science and engineering, XRD has become integral to state-of-the-art techniques, playing a crucial role in qualitative and quantitative phase analyses, examinations of crystallographic textures, and measurements of residual stress. X-ray diffraction capitalizes on the dual wave/particle nature of X-rays, offering detailed insights into the structure of crystalline materials. The XRD works by following the Brag's Law:

$2d\sin\theta = n\lambda$

d = distance between two crystalline lattice planes
θ = the angle of incident / diffracted wave
λ = wavelength of the wave

Furthermore, any articles about nanotechnology and nanoparticles, specially metal based, is considered incomplete, until it has XRD in it, since it is also regarded as the most basic and first characterization technique that confirms that phase, crystal structure and crystalline size of the nanoparticles. **Figure 2.3 (a)** contains the working principle of XRD and **(b)** in-set contains the recorded XRD patterns of IO and IO@TiO_2 **(b)** is adopted from [22], published under open access, Creative Commons (*CC*) 4.0.

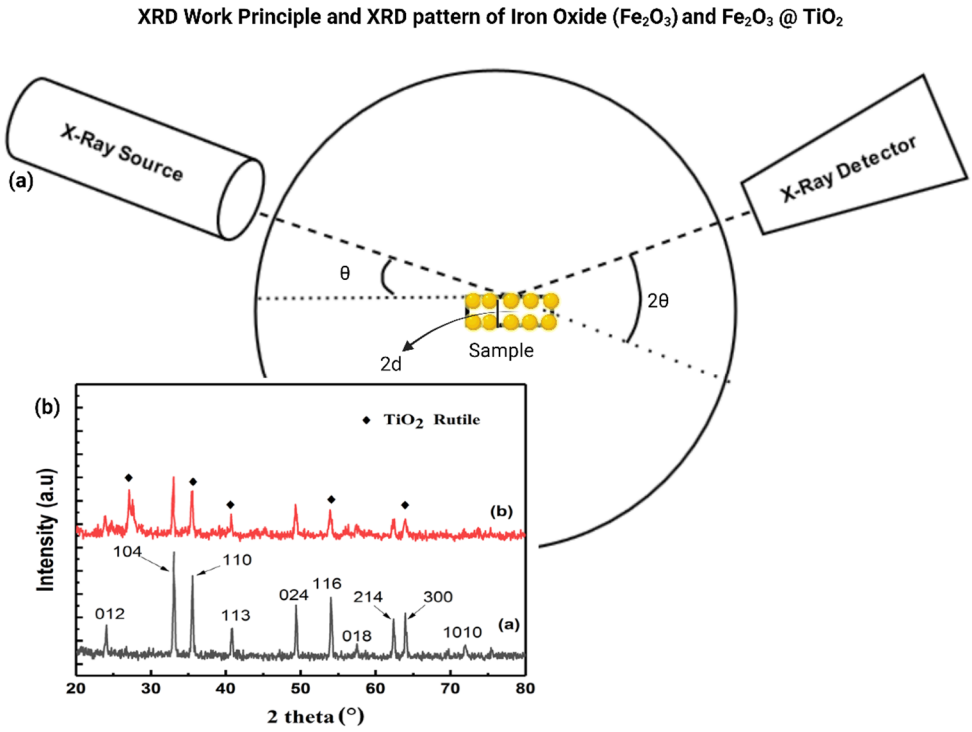

FIGURE 2.3
Working principle of XRD and XRD pattern. (a) Working principle of XRD (b) XRD pattern obtained for Fe_2O_3 and Fe_2O_3 @ TiO_2, (b) is adopted from [22], published under open access, Creative Commons (*CC*) 4.0.

DLS

Dynamic light scattering (DLS), also known as photon correlation spectroscopy or quasi-elastic light scattering, serves as a non-invasive method for sizing particles and molecules within a suspension [23]. This technique revolves around the measurement of the speed of particles engaged in Brownian motion, a phenomenon influenced by various factors such as temperature, viscosity and particle size. At its core, DLS involves the time-resolved assessment of coherent light scattered by objects like large molecules or fine particles. The measurement signals are scrutinized for fluctuations, primarily attributed to the thermal motion of scattering objects, occurring at relatively small-time scales – often in microseconds and even nanoseconds. For instance, DLS facilitates the exploration of vibrations in particle networks, enabling the study of phase transitions in colloidal suspensions [24] and the quantification of elastic properties in gels [6].
In more technical terms, DLS utilizes a monochromatic light beam, like a laser, which interacts with a solution containing sample, causing them to follow Brownian motion. This motion induces a change in the wavelength of the incident light, known as the Doppler shift, and this alteration is correlated with the size of the particles. **Figure 2.4** shows the Typical schematics of a DLS, the figure is insipid

from [22]. The diffusion coefficient of the particles, measured through their Brownian motion, along with the autocorrelation function, allows for the calculation of the sphere size distribution. DLS observes variations in scattered intensity over time at a fixed scattering angle (typically 90 degrees), in contrast to static light scattering, which explores scattered intensity as a function of angle. As molecules diffuse with Brownian motion in relation to the detector, interference occurs, leading to fluctuations in light intensity. By measuring the timescale of these fluctuations, DLS becomes a valuable tool for providing insights into the average size, size distribution, and polydispersity of molecules and particles in solution [25].

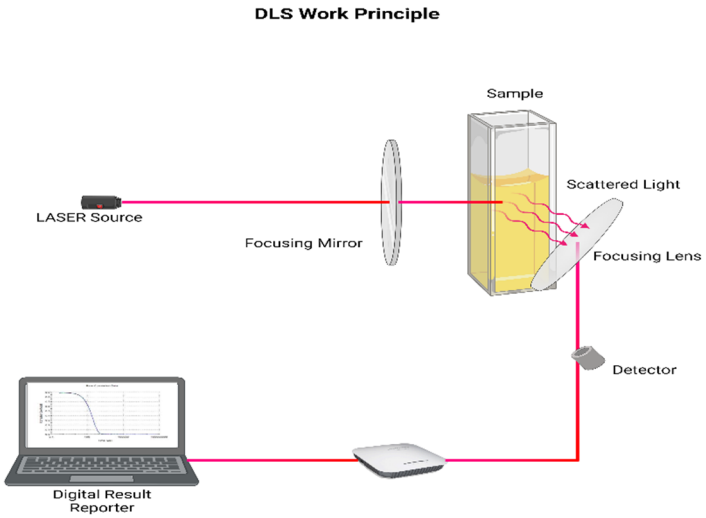

FIGURE 2.4
Typical work principle of a DLS.

In terms of advantages, DLS offers a short experimental duration and modest development costs. However, it comes with disadvantages such as being time-consuming, particularly for slow dynamics, applicable only to transparent samples, sensitivity to mechanical disturbances, and a relatively low signal strength. Its applications span diverse areas, providing size information for particles like proteins, polymers, micelles, carbohydrates, and nanoparticles (NPs). The mean effective diameter of particles can be determined, dependent on factors like the particle core size, surface structures, particle concentration, and types of ions in the medium.

CLSM

Confocal Laser Scanning Microscopy (CLSM) has emerged as a pivotal advancement in fluorescence imaging, revolutionizing biological, and nanobiotechnological research [26]. As a member of the photonic imaging technologies, the term "confocal" denotes image acquisition exclusively from the focal plane, mitigating noise caused by sample thickness optically [27]. In contrast to electron microscopy, CLSM prioritizes specimen preparation speed and compatibility with three-dimensional

(3D) live imaging over resolution, providing valuable insights into dynamic cellular and molecular processes [28]. Laser scanning involves point-by-point image acquisition under localized laser excitation, diverging from the full sample illumination in conventional widefield microscopy [29].

The concept of confocal microscopy traces back to Minsky in the 1950s, with a significant milestone a decade later – the development of the first mechanical scanning confocal laser microscope by Egger and Petran [27]. Evolutions in computer and laser technology facilitated system improvements, leading to the introduction of the first commercial instruments in 1987. CLSM has since become the preferred technique for a new generation researchers [26].

At its core, CLSM analyses fluorescence emitted by a sample following laser beam irradiation. Each fluorescent molecule presents two characteristic spectra: the excitation spectrum exciting the fluorochrome and the emission spectrum corresponding to the emitted wavelengths. CLSM offers numerous advantages in visualizing fluorescent samples over conventional widefield light microscopy, despite some limitations. The primary challenge in conventional epifluorescence microscopy lies in the fluorescence emitted by the wide cone of illumination over a large specimen volume, resulting in reduced resolution and image contrast, especially in thick biological samples [27, 30].

The crux of a confocal microscope is its pinhole, enabling spatial fluorescence filtering. Consisting of a sensing diaphragm and an iris for volume adjustment, confocal microscopes minimize optical pollution by aligning the pinhole size with the Airy disk's diameter. This ensures exclusive information collection from the focal plane, eliminating out-of-focus light. The pinhole's size determines the depth of the in-focus field, influencing the image's optical resolution. **Figure 2.5** shows typical schematics of a CLSM, Figure adopted from [29], published under open access, Creative Commons (*CC*) 4.0. Despite potential drawbacks, including signal loss, phototoxicity, and limited excitation wavelengths, the advantages position the confocal system as a potent tool in biological imaging, offering enhanced resolution and versatile capabilities.

Various advantages of CLSM over traditional imaging techniques include exclusive imaging of the focal plane, suitable penetration for thick specimens, non-invasive optical sectioning for 3D reconstruction, and feasible spectral acquisitions. However, drawbacks encompass potential signal loss, laser-induced phototoxicity, limited excitation wavelengths, and slower mono-focal acquisition. Nonetheless, the benefits establish the confocal system as a robust tool in biological imaging, combining improved resolution with versatile imaging capabilities.

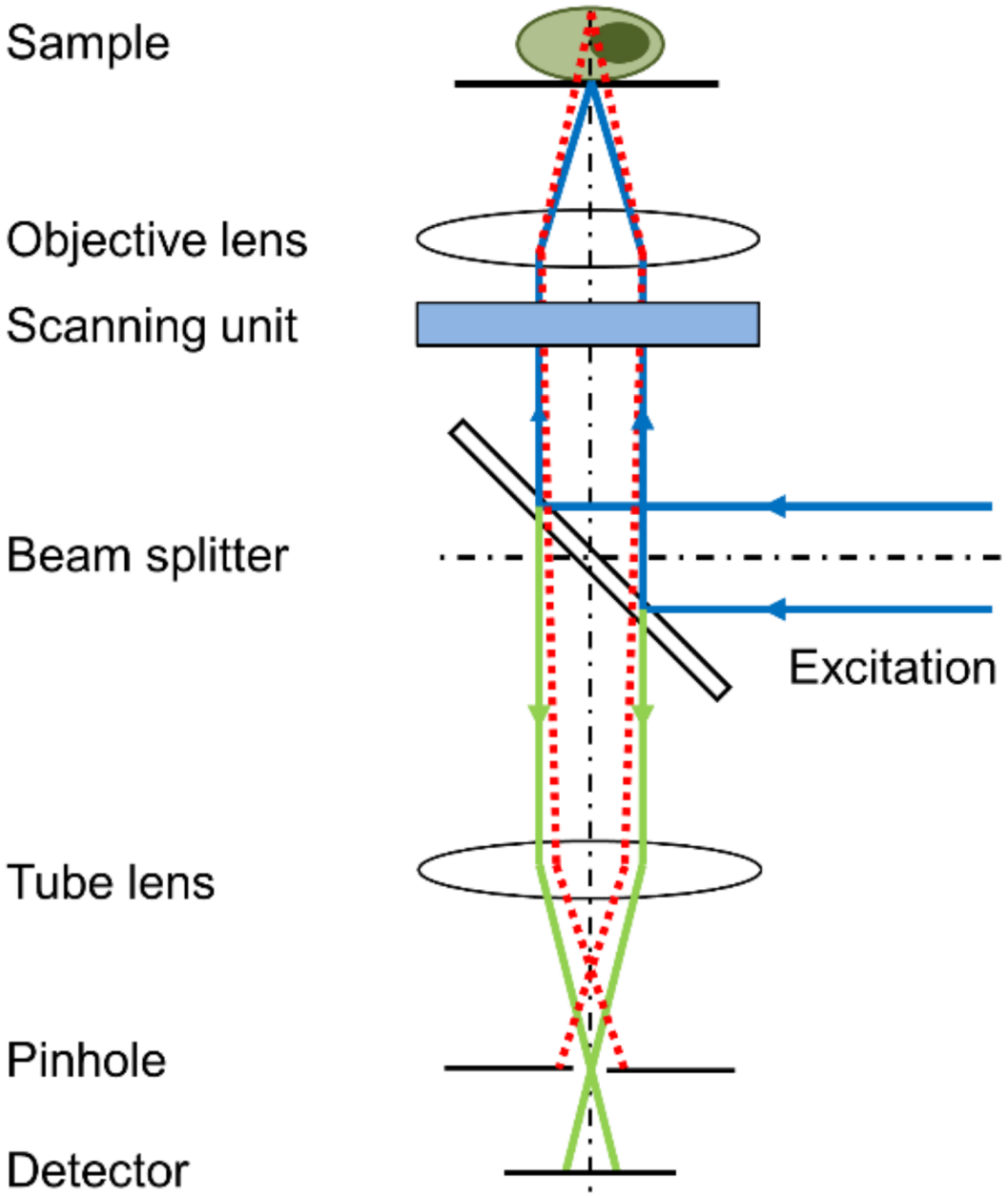

FIGURE 2.5
Schematics of a CLSM, Figure adopted from [29], published under open access, Creative Commons (*CC*) 4.0.

TEM

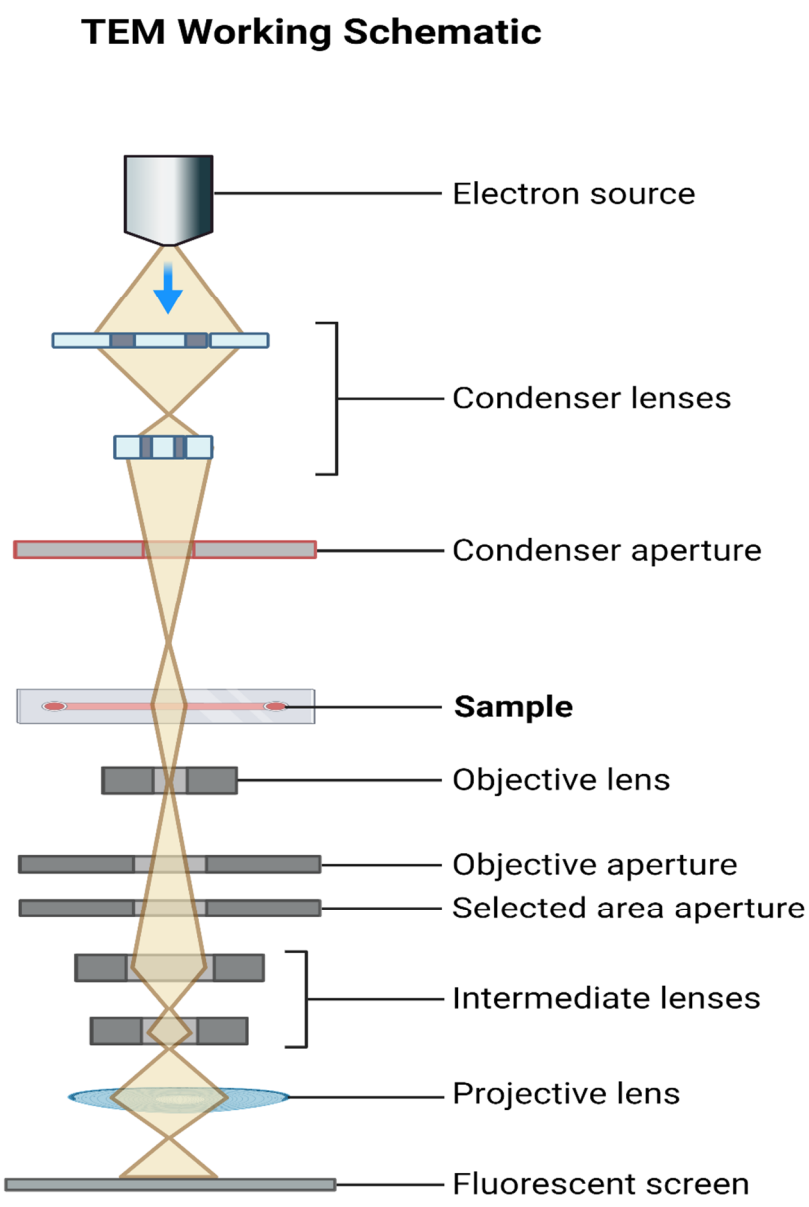

FIGURE 2.6
Scheme of TEM working.

Transmission Electron Microscopy (TEM) utilizes energetic electrons to glean morphological, compositional, and crystallographic details from specimens, distinguishing itself from light

microscopy by employing electronic beam instead of light. The shorter wavelength of electrons, compared to light, affords TEM an exceptional resolution, revealing intricate details down to individual atoms. TEM employs electromagnetic lenses, unlike glass lenses in light microscopy, and presents images on a screen rather than through an eyepiece. **Figure 2.6** shows the scheme of working principle of TEM. While, High-Resolution TEM (HR-TEM), an imaging mode within transmission electron microscopy, facilitates direct visualization of a sample's atomic structure, proving particularly valuable for studying materials on the atomic scale, including semiconductors, metals, nanoparticles, graphene, and carbon nanotubes [31].

Advantages:

- TEM achieves unparalleled magnification, potentially exceeding 1 million times.
- It finds applications across scientific, educational, and industrial domains.
- TEM provides detailed information on elemental and compound structures.
- Images generated are of high quality.
- TEM yields comprehensive data on surface features, shape, size, and structure.
- With proper training, TEM operation is user-friendly.

Disadvantages:

- Transmission electron microscopes are sizable and costly.
- Sample preparation is labor-intensive and may introduce artifacts.
- Specialized training is required for operation and analysis.
- Samples must be electron-transparent, withstand vacuum conditions, and fit chamber size constraints.
- Specialized housing and maintenance are essential for TEM.

Images produced are in black and white.

Application:
TEM serves as a pivotal characterization tool in materials research, especially in the investigation of nanomaterials. Its ability to provide atomic-scale insights makes it instrumental in understanding the properties of various materials, including semiconductors, metals, nanoparticles, and carbon-based structures like graphene and carbon nanotubes.

AFM

Atomic Force Microscopy (AFM) serves as an advanced and highly precise tool for the meticulous observation of sample morphology and the quantitative measurement of mechanical properties at the atomic level. Originating in 1986 through the ingenuity of IBM's G. Binnig, C. F. Quate, and C. Gerber at Stanford University, AFM has evolved into the forefront of scanning force microscopy (SFM), surpassing the limitations of traditional microscopes employing light and electron wavelengths [32, 33].

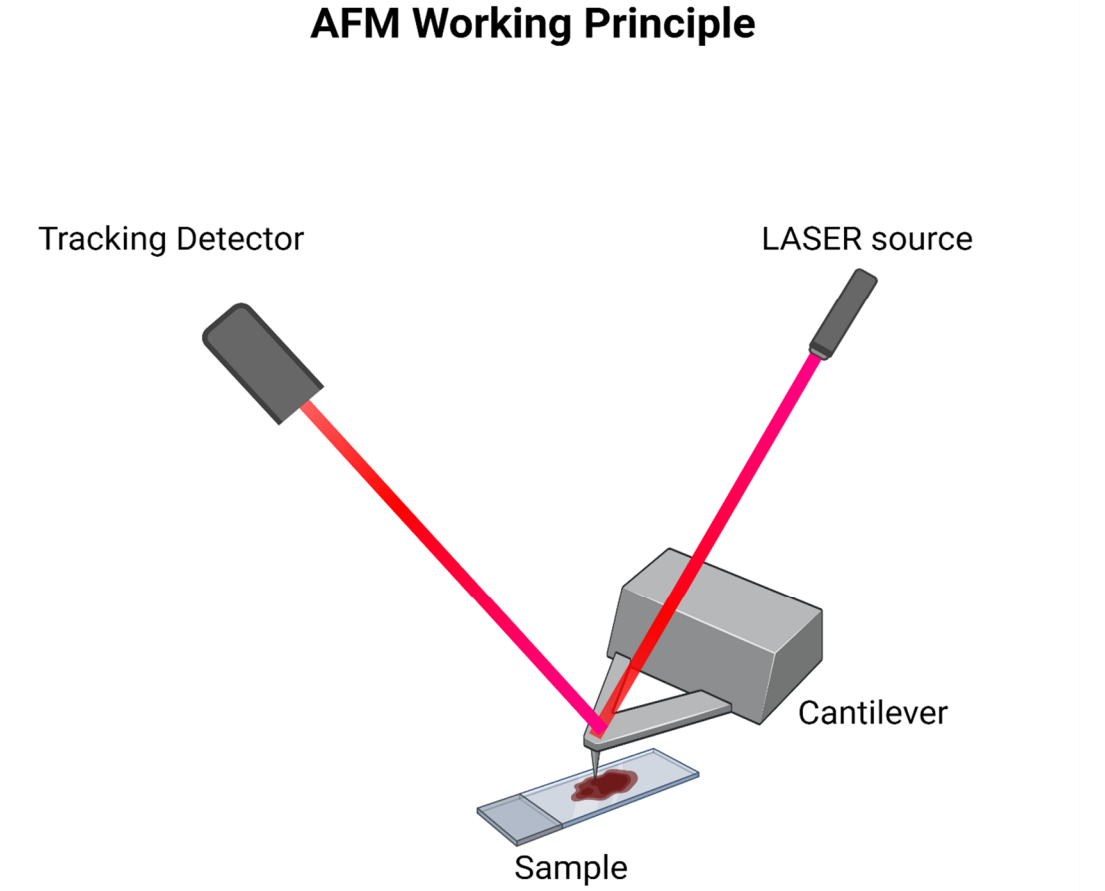

FIGURE 2.7
Simple Pictorial Diagram of AFM working principle.

Key Features and Advantages:

Extremely High Resolution:

- Achieves a horizontal resolution of 0.1 nm, vertical resolution of 0.01 nm, and atomic-level resolution.
- Facilitates direct three-dimensional imaging of molecular and atomic-scale structures.

Straightforward Sample Preparation:

- Minimizes damage to the original structure.
- Allows for an objective and accurate determination of the sample's original appearance.

Observation Under Near-Physiological Conditions:

- Permits the real-time recording of dynamic processes in living cells.
- Offers insights into the behaviour of molecules, organelles, and other structures.

Measurement of Physicochemical Characteristics:

- Capable of measuring intermolecular forces, charge, pH, and other physicochemical properties.

Functionalized Probe for Molecular Identification:

- Utilizes functionalized probes for identifying specific molecules or interaction forces.

These distinctive advantages position AFM at the forefront of applications in biomedicine, clinical medicine, and cancer research. In cancer research, AFM emerges as a crucial tool for measuring cell mechanics, serving as a promising biomarker for indicating cell states [33].

The AFM system comprises essential components, including a micro-cantilever with a probe, a motion detection device, a feedback loop, a piezoelectric ceramic scanning device, and a computer-controlled system for image acquisition and processing [32]. AFM's ability to detect weak interatomic interactions relies on the micro-cantilever's sensitivity to weak forces, which is brought into proximity with the sample for interaction detection. **Figure 2.7** contains pictorial diagram of AFM working principle.

The AFM scanner's multidirectional movement in the X, Y, and Z directions allows comprehensive scanning, providing surface structure information with nano-meter resolution. Using the Hertz model, the Young's modulus value of samples, such as cells and tissues, can be accurately measured, offering valuable insights into the sample's susceptibility to deformation [34].

AFM's imaging and mechanical property detection principle is rooted in the attractive and repulsive forces between atoms. Diverse imaging modes, including contact mode, non-contact mode, and tapping mode, cater to specific advantages, especially for observing surface ultrastructure in biological samples [35]. These capabilities collectively position AFM as a versatile and powerful tool across various scientific disciplines.

SEM

Scanning Electron Microscopy (SEM) finds its origins in the 20th century, with physicists Knoll and Ruska building the first electron microscope in 1933 [36]. The transmission electron microscope (TEM) was improved in 1938 by Von Ardenne, who incorporated a scanning coil, leading to the development of the scanning transmission electron microscope (STEM) [37]. Operating at 23 kV with 8000x magnification and a 50-100 nm resolution, Ardenne's creation set standards for subsequent SEM systems, although a lab explosion prevented its commercialization [38].

In 1942, Zworykin, Hillier, and Snyder proposed a new description for SEM, emphasizing secondary electron emission for topographic contrast. Oatley and McMullan's work in 1952 led to the electrostatic lens SEM at 40 kV, further advanced by Smith's signal processing and double deflection scanning. O. Wells introduced stereoscopic pairs in 1953 for 3D micrograph examination, while Everhart and Thornley developed the scintillator detector, enhancing signal-to-noise ratio [39].

By 1963, Pease's SEM V system became the first commercially available instrument, known as "Stereoscan." Advances included improved electron sources, and the energy-dispersive spectrometer (EDS) was invented in 1968 [38]. SEM's evolution continued, with Danilatos' study from 1991 to 1993 resulting in an instrument capable of examining both wet and dry specimens. Current

SEMs utilize digital image generation, equipped with EDS systems and modern software for efficient data analysis [39].

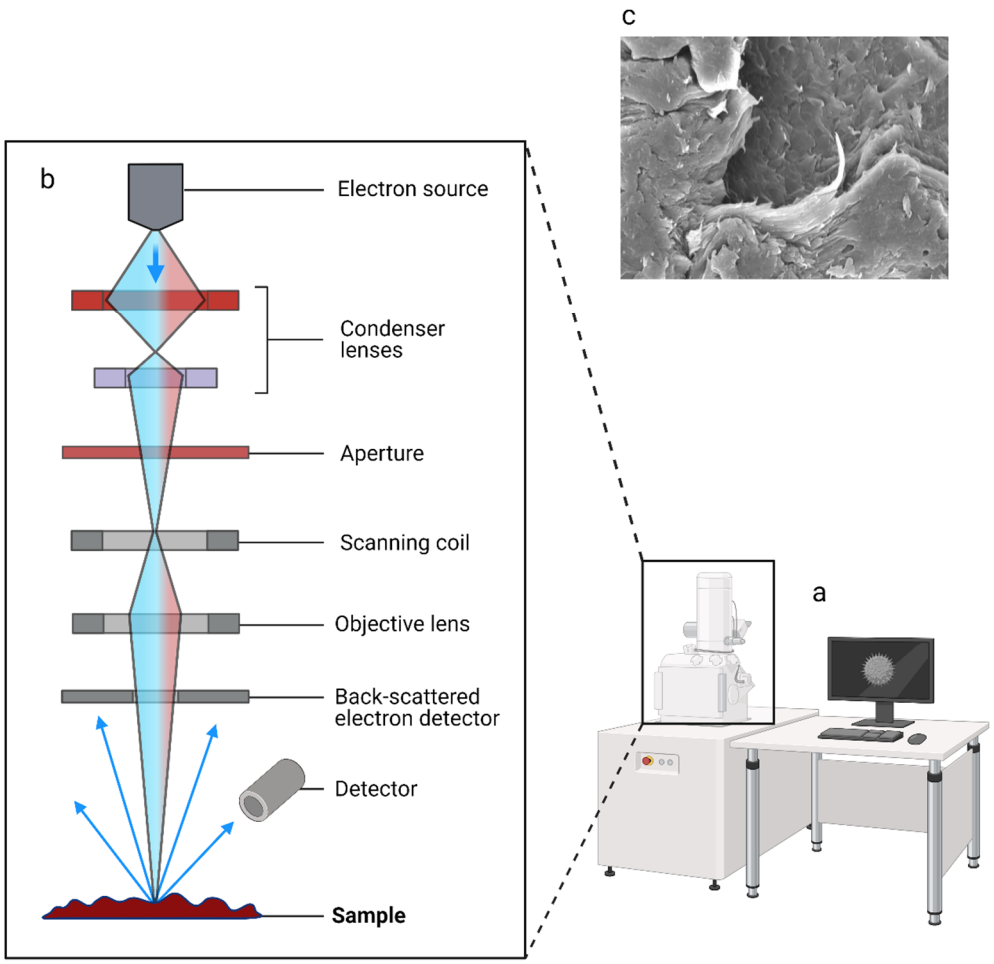

FIGURE 2.8
Information from setup to image collected from SEM. (a) Typical setup of SEM instrument (b) The pictorial diagram of SEM working principle and (c) Sample of image collected from SEM analysis.

SEM applies a high-energy electron beam, typically ranging from 100 to 30,000 electron volts [40]. Lenses compress the initial spot size, and SEMs have a spot size of less than 10 nm. Electrons interact with the specimen, generating signals for image production. Scan coils create a raster on the specimen's surface, and magnification depends on the working distance, automatically adjusted in modern SEMs [39]. A typical SEM setup can be seen in **Figure 2.8(a)**. while in set **(b)**, shows the pictorial schematics of SEM working principle and inset **(c)** SEM obtained image can be seen. In the obtained results, the dark spots give information about indents or pores in the surface, while the bright spots identify the peaks or risen spots on the analysed surface.

An electron detector captures emitted electrons (signals) from the scanned sample, and both secondary electrons (SE) and backscattered electrons (BSE) contribute to image production. A Scintillator detector can be used for both SE and BSE. The signals are displayed on a viewing screen, with operators controlling brightness and intensity. High magnification, beyond 10,000x, is often used for small details within the specimen [41].
The SEM image's partly three-dimensional nature depends on visualizing the topography, influenced by the number of BSE and SE. The angle of inclination of the sample surface affects topographic contrast, with an inclination exceeding 50º up to 70 enhancing both BSE and SE signals [39].
The Sem's usually come with an attached instrument called EDS. EDS stands for Energy Dispersive Spectrum, which gives information about elemental composition of the sample. We will discuss about EDS in next topic.

EDS

Within Scanning Electron Microscopy (SEM), the analysis of x-rays involves a detailed procedure encompassing various crucial steps. These steps collectively contribute to a comprehensive understanding of a specimen's composition, from its qualitative features to quantitative details.
The analytical process within Scanning Electron Microscopy (SEM) unfolds in a systematic manner, comprising several key stages. It begins with a qualitative analysis of the sample, an initial step that facilitates the identification of the various elements present within it. Subsequently, a critical consideration arises in determining the problem or purpose of the analysis, emphasizing whether the focus is on measuring composition gradients or comprehending the sample's chemical composition. Following this, sophisticated software is deployed to execute quantitative corrections, generating numerical concentration results that contribute to a comprehensive quantitative understanding of the specimen's composition.
A pivotal prerequisite for accurate analysis is emphasized in ensuring the polished sample is stored in a dry environment before examination, mitigating the risk of potential contamination on its surface. The subsequent step involves meticulous sample preparation, necessitating the sample to be flat, polished, and with a thickness less than 0.1 µm, ensuring it remains invisible under the microscope [39].
The analytical journey culminates in the quantitative analysis, where the x-ray intensities of each element in the sample are measured. This final step is of paramount importance, serving as a linchpin for extracting valuable information about the specimen. In essence, the outlined sequence, from qualitative analysis to quantitative assessment, forms a cohesive and rigorous framework for SEM analysis, contributing to a thorough exploration of the composition of specimens [39].
This intricate sequence of steps, from problem determination to quantitative analysis, forms the foundation of SEM analysis equipped with Energy-Dispersive Spectrometer (EDS) capability.
Figure 2.9 provides a pictorial image of the EDS working principle. The EDS detector efficiently separates characteristic x-rays of various elements within the sample into an energy spectrum.

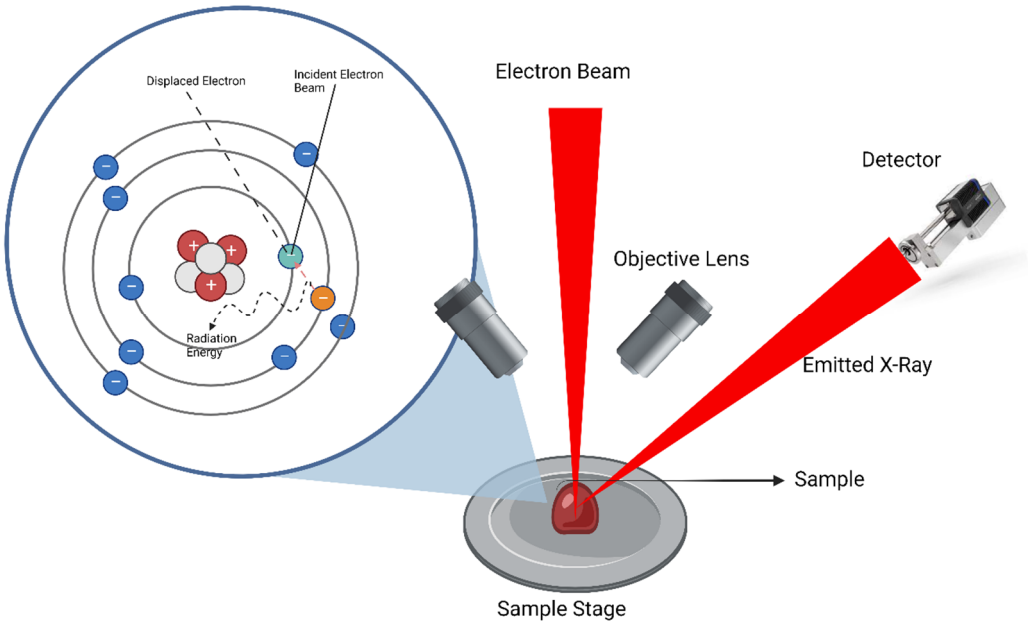

FIGURE 2.9
In detail schematic working principle of EDS.

X-rays are generated as the electron beam emitted from the gun penetrates and interacts with the volume beneath the sample's surface. This phenomenon is rooted in well-defined physics principles, where electrons entering the Coulomb field of a specimen decelerate, leading to the emission of photon energy. In SEM analysis, this principle results in the emission of characteristic x-rays, each energy specific to the elements present in the specimen.
The process of quantification, crucial for meaningful analysis, traces back to Heinrich's 1968 publication on "Quantitative Electron Probe Microanalysis [42]." Despite challenges, Heinrich's seminal work established a standard quantification scheme, ultimately leading to the development of EDS. Heinrich, a key contributor, played a pivotal role in introducing EDS to the x-ray field, with subsequent studies focusing on software development and reference materials for microanalysis standards [43]. Through the outlined steps, SEM equipped with EDS capability emerges as a powerful tool for exploring specimen composition, offering both qualitative and quantitative insights. From initial problem identification to final numerical concentration results, this comprehensive approach ensures the robustness and accuracy of the analytical process in the realm of electron microscopy.

Conclusion

Apart from these characterization techniques, there is a vast number of instruments available to analyse various structural, morphological, elemental, and even electronic and electronic spin behaviour related properties of the nanoparticles, but we have looked over the most important and basic tools, that are used in Nanomaterial analysis.

References

1. Sani, A., et al., *Floral extracts-mediated green synthesis of NiO nanoparticles and their diverse pharmacological evaluations.* Journal of Biomolecular Structure and Dynamics, 2021. **39**(11): p. 4133-4147.
2. Hassan, D., et al., *Biosynthesis of pure hematite phase magnetic iron oxide nanoparticles using floral extracts of Callistemon viminalis (bottlebrush): their physical properties and novel biological applications.* Artificial Cells, Nanomedicine, and Biotechnology, 2018. **46**(sup1): p. 693-707.
3. Dilawar, H., et al., *Focused Ion Beam Tomography*, in *Ion Beam Techniques and Applications*, A. Ishaq and Z. Tingkai, Editors. 2019, IntechOpen: Rijeka. p. Ch. 5.
4. Mustafa, G., et al., *Nanoscale drug delivery systems for cancer therapy using paclitaxel— A review of challenges and latest progressions.* Journal of Drug Delivery Science and Technology, 2023. **84**: p. 104494.
5. Kumar, A. and C.K. Dixit, *3 - Methods for characterization of nanoparticles*, in *Advances in Nanomedicine for the Delivery of Therapeutic Nucleic Acids*, S. Nimesh, R. Chandra, and N. Gupta, Editors. 2017, Woodhead Publishing. p. 43-58.
6. Jose Chirayil, C., et al., *Chapter 1 - Instrumental Techniques for the Characterization of Nanoparticles*, in *Thermal and Rheological Measurement Techniques for Nanomaterials Characterization*, S. Thomas, et al., Editors. 2017, Elsevier. p. 1-36.
7. Penner, M.H., *Basic Principles of Spectroscopy*, in *Food Analysis*, S.S. Nielsen, Editor. 2017, Springer International Publishing: Cham. p. 79-88.
8. Akash, M.S.H. and K. Rehman, *Ultraviolet-Visible (UV-VIS) Spectroscopy*, in *Essentials of Pharmaceutical Analysis*. 2020, Springer Nature Singapore: Singapore. p. 29-56.
9. Nemeş, N.S. and A. Negrea, *Infrared and Visible Spectroscopy: Fourier Transform Infrared Spectroscopy and Ultraviolet– Visible Spectroscopy*, in *Microbial Electrochemical Technologies*. 2023. p. 163-200.
10. George, G., R. Wilson, and J. Joy, *Chapter 3 - Ultraviolet Spectroscopy: A Facile Approach for the Characterization of Nanomaterials*, in *Spectroscopic Methods for Nanomaterials Characterization*, S. Thomas, et al., Editors. 2017, Elsevier. p. 55-72.
11. Guerrero-Pérez, M.O. and G.S. Patience, *Experimental methods in chemical engineering: Fourier transform infrared spectroscopy—FTIR.* The Canadian Journal of Chemical Engineering, 2020. **98**(1): p. 25-33.
12. Sengupta, S., L. Bromley Iii, and L. Velarde, *Aggregated States of Chalcogenorhodamine Dyes on Nanocrystalline Titania Revealed by Doubly Resonant Sum Frequency Spectroscopy.* The Journal of Physical Chemistry C, 2017. **121**(6): p. 3424-3436.
13. Campanella, B., V. Palleschi, and S. Legnaioli, *Introduction to vibrational spectroscopies.* ChemTexts, 2021. **7**(1): p. 5.
14. Athokpam, B., S.G. Ramesh, and R.H. McKenzie, *Effect of hydrogen bonding on the infrared absorption intensity of OH stretch vibrations.* Chemical Physics, 2017. **488-489**: p. 43-54.
15. Ricci, A., et al., *Application of Fourier Transform Infrared (FTIR) Spectroscopy in the Characterization of Tannins.* Applied Spectroscopy Reviews, 2015. **50**(5): p. 407-442.
16. Berthomieu, C. and R. Hienerwadel, *Fourier transform infrared (FTIR) spectroscopy.* Photosynthesis Research, 2009. **101**(2): p. 157-170.

17. Busch, U., *Claims of priority – The scientific path to the discovery of X-rays.* Zeitschrift für Medizinische Physik, 2023. **33**(2): p. 230-242.
18. Eckert, M., *Disputed discovery: The beginnings of X-ray diffraction in crystals in 1912 and its repercussions.* Zeitschrift für Kristallographie - Crystalline Materials, 2012. **227**(1): p. 27-35.
19. Staufer, T. and F. Grüner, *Review of Development and Recent Advances in Biomedical X-ray Fluorescence Imaging.* International Journal of Molecular Sciences, 2023. **24**(13): p. 10990.
20. Omori, N.E., et al., *Recent developments in X-ray diffraction/scattering computed tomography for materials science.* Philosophical Transactions of the Royal Society A: Mathematical, Physical and Engineering Sciences, 2023. **381**(2259): p. 20220350.
21. Dinnebier, R.E. and S.J.L. Billinge, *Principles of Powder Diffraction*, in *Powder Diffraction: Theory and Practice*, R.E. Dinnebier and S.J.L. Billinge, Editors. 2008, The Royal Society of Chemistry. p. 0.
22. Sultan, H., et al., *Green Synthesis and Investigation of Surface Effects of α- Fe_2O_3@TiO_2 Nanocomposites by Impedance Spectroscopy.* Materials, 2022. **15**(16): p. 5768.
23. Xu, R., *Light scattering: A review of particle characterization applications.* Particuology, 2015. **18**: p. 11-21.
24. Salamanca-Buentello, F., et al., *Nanotechnology and the Developing World.* PLOS Medicine, 2005. **2**(5): p. e97.
25. Brar, S.K. and M.P. Verma, *Measurement of nanoparticles by light-scattering techniques.* Trends in Analytical Chemistry, 2011. **30**: p. 4-17.
26. Paddock, S.W., *Confocal Laser Scanning Microscopy.* BioTechniques, 1999. **27**(5): p. 992-1004.
27. Canette, A. and R. Briandet, *MICROSCOPY | Confocal Laser Scanning Microscopy*, in *Encyclopedia of Food Microbiology (Second Edition)*, C.A. Batt and M.L. Tortorello, Editors. 2014, Academic Press: Oxford. p. 676-683.
28. Lidke, D.S. and K.A. Lidke, *Advances in high-resolution imaging – techniques for three-dimensional imaging of cellular structures.* Journal of Cell Science, 2012. **125**(11): p. 2571-2580.
29. Schneckenburger, H. and V. Richter, *Laser Scanning versus Wide-Field—Choosing the Appropriate Microscope in Life Sciences.* Applied Sciences, 2021. **11**(2): p. 733.
30. Stigliano, L., J. Caumartin, and K. Benzerara, *Chapter 6 - Micro- and nanoscale techniques for studying biofilm-mineral interactions*, in *Methods in Microbiology*, V. Gurtler and M. Patrauchan, Editors. 2023, Academic Press. p. 143-192.
31. Hadermann, J., *High-Resolution Electron Microscopy. By John C. H. Spence. Oxford University Press, 2013. Pp. 406. Price £75. ISBN: 978-0-19-966863-2.* Acta crystallographica Section B, Structural science, crystal engineering and materials, 2014. **70**: p. 778.
32. Binnig, G., C.F. Quate, and C. Gerber, *Atomic Force Microscope.* Physical Review Letters, 1986. **56**(9): p. 930-933.
33. Deng, X., et al., *Application of atomic force microscopy in cancer research.* Journal of Nanobiotechnology, 2018. **16**(1): p. 102.
34. Kontomaris, S.V., A. Malamou, and A. Stylianou, *The Hertzian theory in AFM nanoindentation experiments regarding biological samples: Overcoming limitations in data processing.* Micron, 2022. **155**: p. 103228.
35. Moreno-Herrero, F., et al., *Atomic force microscopy contact, tapping, and jumping modes for imaging biological samples in liquids.* Physical Review E, 2004. **69**(3): p. 031915.

36. Mestres Ventura, P., *The electron microscope on the eve of its first centenary.* 2023. **1**: p. 111-127.
37. Liu, J., *Advances and Applications of Atomic-Resolution Scanning Transmission Electron Microscopy.* Microscopy and Microanalysis, 2021. **27**(5): p. 943-995.
38. Goldstein, J.I., et al., *The SEM and Its Modes of Operation*, in *Scanning Electron Microscopy and X-ray Microanalysis: Third Edition*. 2003, Springer US: Boston, MA. p. 21-60.
39. Abdullah, A. and A. Mohammed, *Scanning Electron Microscopy (SEM): A Review*. 2019.
40. Ul-Hamid, A., *Imaging with the SEM*, in *A Beginners' Guide to Scanning Electron Microscopy*. 2018, Springer International Publishing: Cham. p. 129-180.
41. Sutton, M.A., et al., *Scanning Electron Microscopy for Quantitative Small and Large Deformation Measurements Part I: SEM Imaging at Magnifications from 200 to 10,000.* Experimental Mechanics, 2007. **47**(6): p. 775-787.
42. Heinrich, K.F., *Quantitative electron probe microanalysis: proceedings of a seminar held at the National Bureau of Standards, Gaithersburg, Maryland, June 12-13, 1967*. 1968: US National Bureau of Standards.
43. Friel, J.J. and C.E. Lyman, *Tutorial Review: X-ray Mapping in Electron-Beam Instruments.* Microscopy and Microanalysis, 2006. **12**(1): p. 2-25.